ROLE OF ASTROCYTIC EPHRIN-B1 IN SYNAPTOGENESIS IN THE DEVELOPING HIPPOCAMPUS

By

Sandy Ayman Shoukry Hanna

A capstone project submitted for
Graduation with University Honors

April 18, 2017

University Honors
University of California, Riverside

APPROVED

_____

Dr. Iryna Ethell
Department of Biomedical Sciences

_____

Dr. Richard Cardullo, Howard H Hays Jr. Chair and Faculty Director, University Honors
Interim Vice Provost, Undergraduate Education

Abstract

Ephrin-B1 is known to be expressed by neurons and to influence cell adhesion and development of the circuits in the nervous system through its interactions with neuronal EphB receptors. Recent studies in our lab suggest that ephrin-B1 is also expressed in astrocytes and is involved in regulating synaptic responses in the adult mouse hippocampus through glial-neuronal interactions. Astrocyte-specific deletion of ephrin-B1 resulted in an increase in the number of silent synapses. Images of dendrites in the CA1 hippocampus of ephrin-B1 knockout mice also showed abundance of immature dendritic spines, sites of the silent synapses. The study indicates that astrocytic ephrin-B1 is involved in pruning of the silent synapses to maintain mature and functional synaptic network in the adult hippocampus. In this study, we will be assessing the effects of knocking out ephrin-B1 in developing hippocampal astrocytes at postnatal days (P) 14. Astrocytic ephrin-B1 deletion will be achieved by crossing homozygous floxed ephrin-B1 female mice with Cre-GFAP-ERT2 male mice, followed by tamoxifen injection to induce ablation of astrocytic ephrin-B1 in the developing brain at P14. Synapses and dendritic spines will be analyzed in the striatum radiatum layer of the CA1 hippocampus of 100-micron coronal brain sections obtained at P28. We predict that astrocytic ephrin-B1 is also involved in the synapse removal during development and ephrin-B1 deletion from astrocytes will result in excessive formation of spines and synapses in the developing hippocampus. In contrast to the effects of ephrin-B1 deletion in the adult hippocampus, we expect an increase in synaptic responses and mature spines in the developing hippocampus during the process of active formation of new synaptic connections.

Acknowledgements

I am heartily thankful for my mentor, Dr. Iryna Ethell, for her encouragement, support, and guidance throughout the completion of project.

I am thankful for Amanda Nguyen and Jordan Koeppen for the helpful revisions and discussions, and for Koeppen's contributions of previously collected data to serve as reference in some of the comparisons made in this project.

I would also like to thank all the Ethell lab members for their various contributions.

This work was supported by the NIH grant MH067121.

Table of Contents

List of Figures

Introduction

Role of Astrocytic ephrin-B1 in Synaptogenesis in the Developing Hippocampus

Synapses are the connections neurons form with each other to communicate; in a single synapse, one neuron is transmitting a signal – the presynaptic neuron – and another neuron is receiving the signal – the postsynaptic neuron. The presynaptic neuron releases vesicles containing a neurotransmitter, i.e. the chemical messenger, through the synaptic terminals [synaptic boutons] of its axon. On the other end of the synapse, the postsynaptic neuron receives the signal through its dendrites, where small protrusions on the dendrite – the dendritic spines – are sometimes involved in receiving the signals, such as in receiving excitatory signals (Harris, 1999). Recent discoveries suggested that a third party, astrocytic glial cells, regulates communications between neurons at the synapse. One way astrocytic regulation of synapses may be carried out is through its modulation of bidirectional signaling between ephrins and EphB receptors (Henkemeyer, 2003; Murai, 2004; Kayser, 2006). Ephrins are membrane bound ligands that bind to a receptor tyrosine kinase (RTK) known as Erythroprotein-producing hepatocellular carcinoma (Eph). There are two known classes of Eph receptors (EphA and EphB) and they differ in their affinity of binding ephrin-A versus ephrin-B ligands (Gale, 1996; Egea, 2007; Qin, 2010; Kao, 2011). Bidirectional signaling between ephrins and Eph receptors consists of forward signaling, from the ephrins to the Eph receptors, and reverse signaling from the Eph receptors to ephrins (Xu, 1999; Kao, 2011). This model of signaling has been suggested to play a role in the establishment of multiple circuits in the nervous system. For instance, neuronal ephrin-Eph bidirectional signaling has been shown to contribute,

through attractive and repulsive cues, to axon guidance in motor neurons, establishing precise innervation of limb muscle by the neurons (Xu, 1999; Kao, 2011).

Circuit regulation by neuronal ephrin-Eph bidirectional signaling has also been found in the hippocampus. Researchers found that different types of ephrin and Ephs are expressed in different regions of the hippocampus and contribute to the development of synapses on both the pre-and post-synaptic sites in their respective regions as shown in Figure 1.1 by Hruska and Dalva (2012). One example of neuronal ephrin-Eph regulation of circuits in the hippocampus is ephrinA/EphA role in refining synaptic connections in the CA1-CA3 pryramidal axons. Ephrin-A5 is activating BDNF-induced synapse formation on the presynaptic end, while inhibiting it on the post-synaptic end leading to fine-tuning of the synaptic connections in the pathway (Gottschalk et al., 1999; Marler et al., 2008; Guellmar et al., 2009). Another example of circuit regulation through neuronal ephrin-Eph interactions is found in the stratum radiatum (SR) layer of the CA1 region in hippocampus, where the interactions are suggested to regulate the innervation of CA1 neurons by schaffer collaterals of CA3 neurons (figure 1.2) (Ethell et al. 2001; Henderson et al., 2001; Takasu et al., 2002; Henkemeyer et. al., 2003; Grunwald et al., 2004). Ephrin-B is suggested to regulate the formation of excitatory synapses in the SR region of CA1 hippocampus through its interactions with synaptic EphB receptors (Grunwald et al., 2004). It is also suggested to be regulating the morphology of dendritic spines at the postsynaptic neurons, where knockout EphB receptor prevents maturation of spines (Ethell, 2001). However, the effects of astrocytic of ephrinB-1 interactions with neuronal EphB receptor on the synaptogenesis at the SR region of the CA1 hippocampus were not

studied and will be the focus of this project, where we will assess the extent of these effects during development.

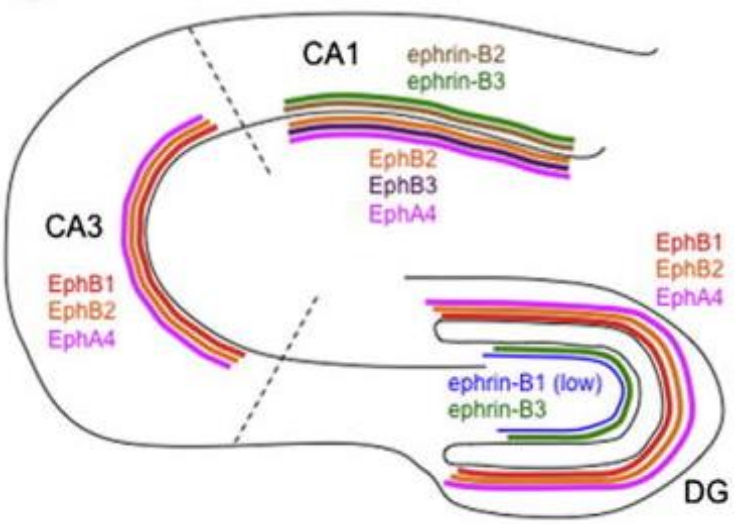

Figure 1.1 Mapping of the expression of Ephs and ephrins in the hippocampus. A depection summerizing most known regional-specific expression of ephrins and Eph receptors in the hippocampus based on the review by Hruska and Dalva (2012).

Ephrin-Eph interactions have been shown to be regulating the morphology of dendritic spines at postsynaptic neurons, in vitro (Ethell and Yamaguchi, 1999; Ethell, 2001; Henkemeyer et al., 2003). Our lab previously compared cultures of wild type (WT) hippocampal neurons and knockout (KO) hippocampal neurons, where knockout neurons were deficient in EphB1, B2 and B3 (Henkemeyer et al., 2003). These studies showed that in WT neuron cultures, dendritic spines formed between days 7 and 14, while maturation of the spines continued until day 21 and was marked by a decrease in the spine length along with adoption of a mushroom-like shape that contained polymerized F-actin (Ethell and Yamaguchi, 1999; Henkemeyer et al., 2003). On the other hand, KO neuron cultures showed no spine formation even at day 21, instead, they exhibited long thin protrusions, which were immature and did not contain F-actin clusters (Henkemeyer

et al., 2003). Consequently, the studies aimed to further assess the effects of individual EphB receptors to find which specific EphB receptor is responsible for the effect on spine formation. Thus, the effects of various combinations of EphB receptor KO, e.g. triple KO (EphB1/EphB2/EphB3), double KOs (EphB1/EphB2, EphB2/EphB3, EphB1/EphB3) and single KOs (EphB1, EphB2, EphB3) were compared. The studies showed that double KO mice exhibited an increase in spine length, and they exhibited less mushroom-like spines and more filopodia-like protrusions (Henkemeyer et al., 2003). Furthermore, EphB1/EphB2 double KO, particularly, showed defects in spine formation that were highly comparable to the defects in the triple mutants (Henkemeyer et al., 2003). In vivo studies of EphB triple KO mice, showed decreased spine density and abnormal spine morphology when compared to WT mice, although most of the spines in WT CA3 neurons are mushroom-shaped (thin neck and large head), spines in KO CA3 neurons have very small or without heads (Henkemeyer et al., 2003, p1318). These studies allowed us to understand the role of EphB receptors in synaptogenesis. Further research showed that the ligand of EphB receptors, ephrin-B, also plays a role in maturation of spines and formation of synapses. In vitro studies of hippocampal neurons showed that activation of ephrin-Bs increased number of mature spines, i.e. mushroom-like spines, while inhibition of ephrin-B reverse signaling increased number of immature spines, i.e. long and thin filopodia (Segura et al., 2007). In this study, rat hippocampal neurons were transfected with ephrinB1ΔC to block ephrin-B signaling. EphrinB1ΔC expressed at the cellular membrane and binds EphB receptors of neighboring cells, thereby interfering with binding of the endogenous ephrin-B ligands with their EphB receptors. The researchers transfected the neurons with ephrinB1ΔC on day 7 of their culture and

analyzed spine morphology on day 11. Analysis showed significant increase in spine length and levels of filopodia-like protrusions in the ephrinB1ΔC transfected neurons, in comparison to control-transfected neurons that had intact ephrin-B-EphB signaling. Dendritic spines were analyzed again on day 14 and the same effect were observed; spine length was significantly increased in the ephrinB1ΔC transfected neurons, proportion of filopodia-like protrusions was also significantly increased in ephrinB1ΔC transfected neurons, and consequently, the ephrinB1ΔC transfected neurons had significantly decreased percentage of mature spines in comparison to the control (Segura et al., 2007).

Recent studies in our lab, which aimed to study the role of astrocytes in brain repair after traumatic brain injury (TBI), showed that ephrinB1 was upregulated in astrocytes following TBI which was associated with a decrease in excitatory synapses in the Stratum Radiatum region of the CA1 hippocampus following TBI (Nikolakopoulou et al., 2016). The excitatory synapses were labeled through immunostaining for excitatory presynaptic marker, vGlut1. Their data showed that three days following TBI, ephrin-B1 levels were upregulated in the astrocytes in SR CA1 region of the hippocampus, and this increase in ephrin-B1 was associated with a decrease in vGlut1 labeled presynaptic boutons (Nikolakopoulou et al., 2016). Further in vivo experiments, performed in our lab, demonstrated that knockout of ephrinB-1in adult astrocytes, P70-P90, results a statistically significant increase in excitatory synapses, vGlut1 positive, in the SR CA1 region of hippocampus (Figure 3.1 C), but not inhibitory synapses, GAD65 positive, of the same region (Figure 3.2 C). Ephrin-B1 KO tamoxifen-treated ERT2-CRE^{GFAP} ephrin-B1^{flox} (KO) mice also showed increased spine density, number of spines per 10μm,

(Figure 3.4 A) in comparison to wildtype tamoxifen-treated ERT2-CRE^{GFAP} (WT) mice and increased spine length (Figure 3.3 A).

In this experiment, we aimed to assess the effects of ephrin-B1 in developing mice, P14-P28, both at the pre-synaptic and post-synaptic sites. We injected ERT2-Cre^{GFAP} and ERT2-CRE^{GFAP} ephrin-B1^{flox} mice with tamoxifen at age P14, to obtain WT and ephrin-B1 KO mice, respectively. The animals were perfused at P28 and we obtained coronal sections of the hippocampus (Figure 1.2 B). We carried out similar procedure to that performed in Nikolakopoulou (2016) in labelling excitatory synapses using marker for vesicular glutamate transporter 1, vGlut1; and labeled inhibitory synapses using anti-glutamic acid decarboxylase 65, GAD65. We looked at the effects of ephrin-B1 KO in astrocytes on excitatory and inhibitory synapses formed by schaffer collateral (SC) projections coming from CA3 hippocampus into the CA1 hippocampus at the stratum radiatum (SR) layer (Figure 1.2 C). Furthermore, we examined the effects of ephrin-B1 KO in astrocytes on dendritic spine density and length in CA1 neurons at the SR region of CA1 hippocampus, in tamoxifen treated Thy1-GFP-ERT2-CRE^{GFAP} ephrin-B1^{flox} KO mice. We hypothesize that astrocytic ephrin-B1 is involved in pruning of excitatory synapses during development to allow for formation of few but mature and functional spines, thereby establishing a more refined circuits. We expect an increase in vGlut1 positive puncta in animals lacking astrocytic ephrin-B1 (KO) in comparison to the WT animals, yet, we do not expect to see significant changes in the inhibitory synapses, marked by GAD65. We also expect to see increased spine density, i.e. number of spines per 10μm of dendrite, in the astrocyte-specific ephrin-B1 deficient animals, and increased dendritic spine length.

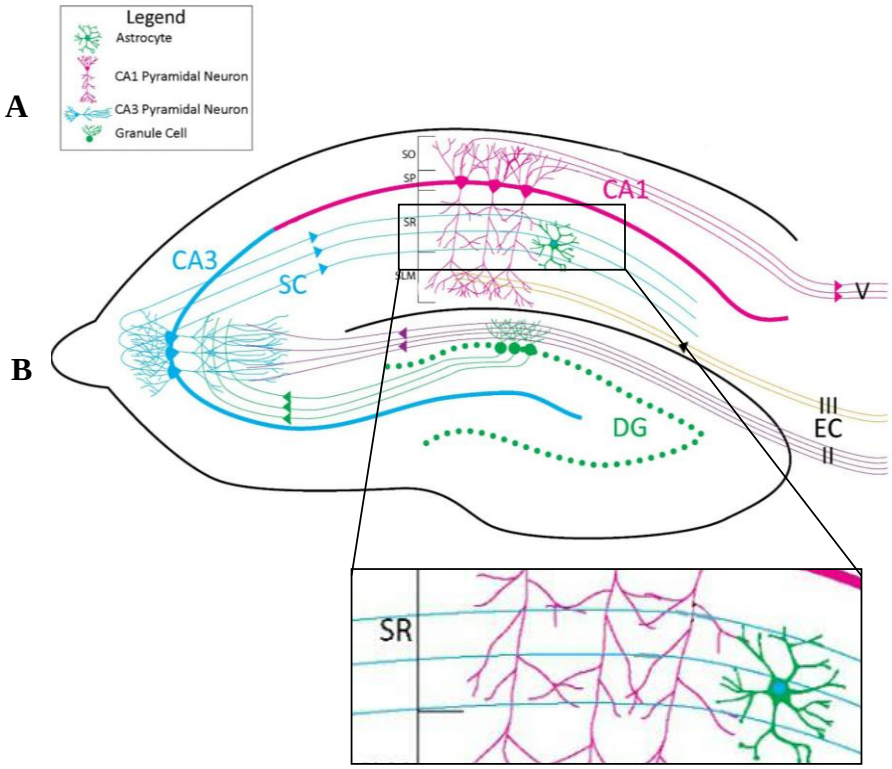

Figure 1.2. Schematic of coronal view of pathways in CA1 region of hippocampus. (A) Figure legends. (B) Coronal section of the hippocampus. (C) Stratum Radiatum region of CA1.

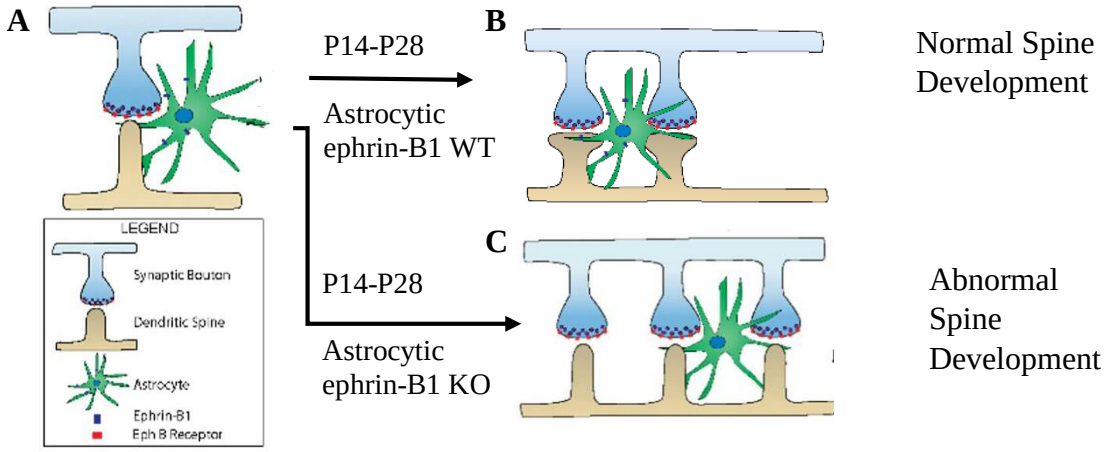

Figure 1.3. Pruning of synapses by astrocytic ephrin-B1 in SR region of CA1 hippocampus, (A) P14 dendritic spines (B) normal spine development into mature spines, i.e. mushroom-like, fewer number of spines in WT mice at P28. (C) immature spines, filopodia-like, larger number of spines in KO mice at P28.

Materials and Methods

Mice and Tamoxifen Injections

In order obtain the knockout mice (KO) and wildtype mice (WT), ERT2-Cre^{GFAP} (Jax#012849) male mice were crossed with ephrin-B1$^{flox/+}$ female mice. The ephrin-B1 $^{flox/+}$ female mouse model are mutant mice which possess one copy of X chromosome with loxP sites flanking exons 2 through 5 of our target gene, i.e. the efnb1 gene encoding for ephrin-B1 (Jax#007664). Upon crossing the ephrin-B1$^{flox/+}$ female mice with ERT2-CRE^{GFAP} male mice, the male offspring will be ERT2-Cre^{GFAP} (WT) or ERT2-Cre^{GFAP} ephrin-B1^{flox} (KO) mice, the latter mice will have exons 2 through 5 of the efnb1 gene floxed by loxP sites.

At age P14 knockout (KO) and wildtype (WT) littermates received daily IP dose of 0.1 mL tamoxifen injections for five consecutive days (Figure 1). Mice were anesthetized with isoflurane and injections were delivered to the IP area. Injections were composed of 0.5 mg of Tamoxifen dissolved at 5mg/mL in 1:9 ethanol/sunflower seed oil. Tamoxifen was expected to lead to deletion of the efnb1 gene, encoding for ephrin-B1, in the ERT2-CRE^{GFAP} ephrin-B1^{flox} (KO) mice. Tamoxifen does so through the activation of ERT2 in the ERT2-CRE^{GFAP} ephrin-B1^{flox} (KO) mice, ERT2 leads to the expression of CRE in astrocytes which excises the target gene located between the two loxP sites, as shown in Figure 2.

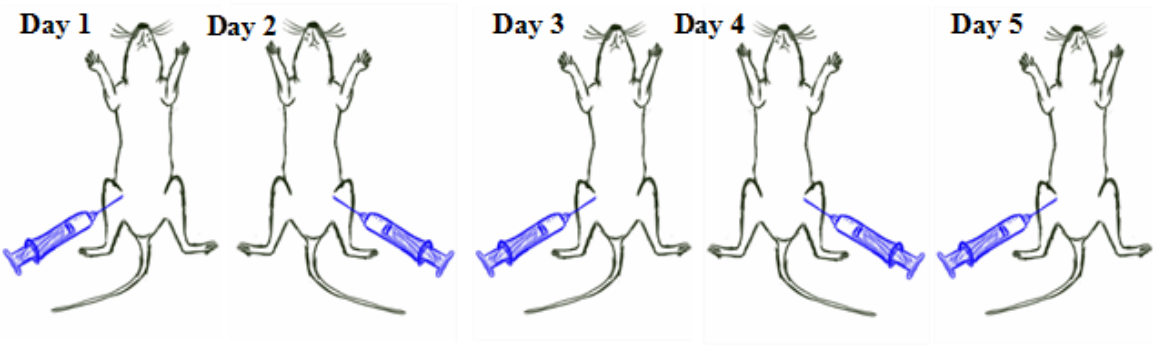

Figure 2.1. Administering Tamoxifen Injection at P14. A dose of 0.1 mL of tamoxifen (0.5 mg of Tamoxifen dissolved at 5mg/mL in 1:9 ethanol/sunflower seed oil) was delivered IP. Injections were intra-exchanged between the left and right side on daily basis as shown in Day 1-5.

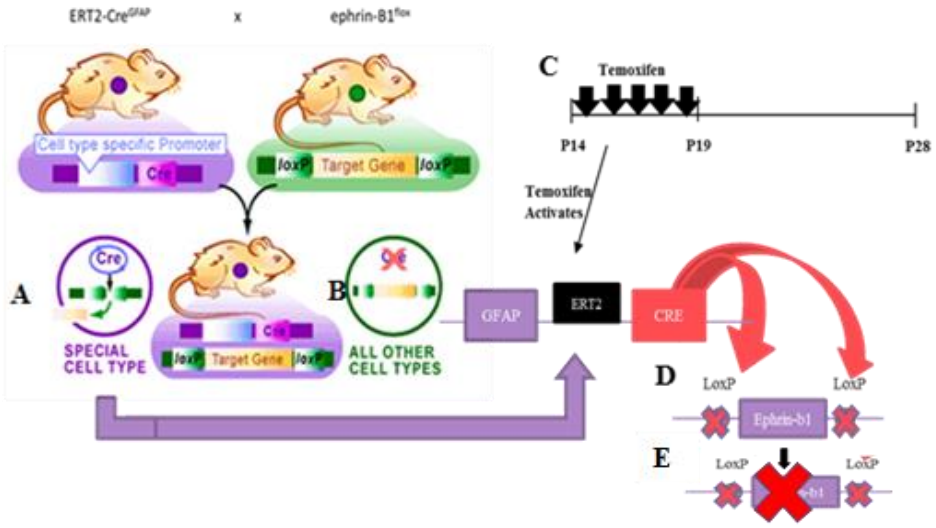

Figure 2.2. Excision of ephrin-B1 in ERT2-CRE^{GFAP} ephrin-B1^{flox} (KO) mice. Breeding of ERT2-CRE^{GFAP} male mouse and ephrin-B1$^{flox/+}$ female mouse yields ERT2-Cre^{GFAP} ephrin-B1^{flox} (KO) in (A) astrocytes but not in (B) other cell types, (C) after an injection of tamoxifen at P14 for five days. (D**)** Tamoxifen activates ERT2 causing CRE to excise the gene encoding for ephrin-B1 located between the loxP sites in the ERT2-Cre^{GFAP} ephrin-B1^{flox} (KO) mice. (E) Ephrin-B1 deletion after excision by CRE at the loxP sites.

Immunohistochemistry

Mice were transcardially perfused at age P28. Perfusion protocol was approved by IACUC; mice were anesthetized using Isoflurane. A procedure similar to what is described in Gage (2012) was employed. Using forceps, we lift skin, then a small incision was made midway through the abdomen. We extended the incision bilaterally across the abdomen and bilaterally upwards towards the arms. Connective tissue was cut until heart was exposed. Using scissors, we cut the right atrium to release blood, then we injected 15 mL of 0.1 M Phosphate Buffered Saline (PBS), pH=7.4, followed by 20 mL of 4% Paraformaldehyde (PFA). The purpose of this procedure is to clear blood from all tissues of the mouse, including brain tissue, using PBS; then fix the tissues using paraformaldehyde. By injecting solutions into the left ventricle of the heart we ensure that the solutions reach all tissues. Brain was extracted as described in Gage (2012) and post-fixed in PFA for 2 hours, then transferred to PBS and stored at 4°C. Coronal sections of 100µm thickness were collected using a vibratome.

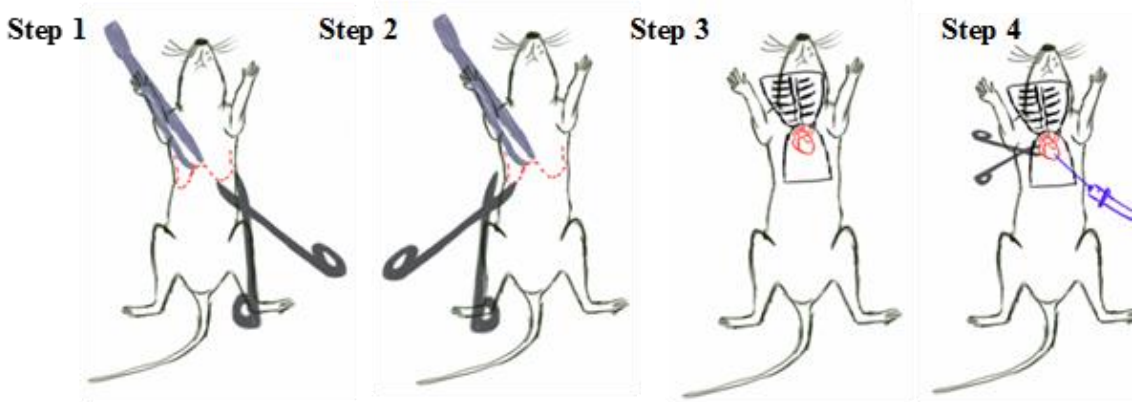

Figure 2.3. Transcardial prefusion procedure (Steps 1-5). Clearing and fixing brain using phosphate buffered saline (PBS) and paraformaldehyde (PFA), respectively.

In order to assess the effects of astrocytic ephrin-B1 deletion on synaptogenesis, we used immunostaining to label for excitatory and inhibitory synapses. Excitatory synapses were labeled through labeling vesicular glutamate transporter 1 (vGlut1) which is an excitatory synapse marker. We used rabbit anti-vGlut1 antibody (1mg/4ml; 482400; Invitrogen). On the other hand, the inhibitory synapses were labeled using mouse anti-glutamic acid decarboxylase 65 (GAD65) antibody (10μg/ml; 559931; BD Pharmingen). We used Fluor 594-conjugated donkey anti-mouse IgG (4 mg/ml; Molecular Probes) to detect GAD65, and Alexa Fluor 488-conjugated donkey anti-goat IgG (4 mg/ ml; Molecular Probes) to detect vGlut1. When mounting our sections we used Vectashield mounting medium containing DAPI (Vector Laboratories Inc.).

Confocal Imaging and Analysis

Confocal images of GAD65 and vGlut1 stains in the stratum radiatum (SR) region of the CA1 hippocampus were obtained using a Leica SP2 confocal laser-scanning microscope. We collected series of high-resolution optical sections (1024x1024-pixel format) using 40x water-immersion objective, 1 zoom at 1-μm step intervals (z-stack of 19 optical sections). Each z-stack was collapsed into a single image and converted into a tiff file and analyzed using Fiji- Image J Software. Each image was threshold-adjusted to identical levels (0-120 intensity) which was measured using ImageJ.

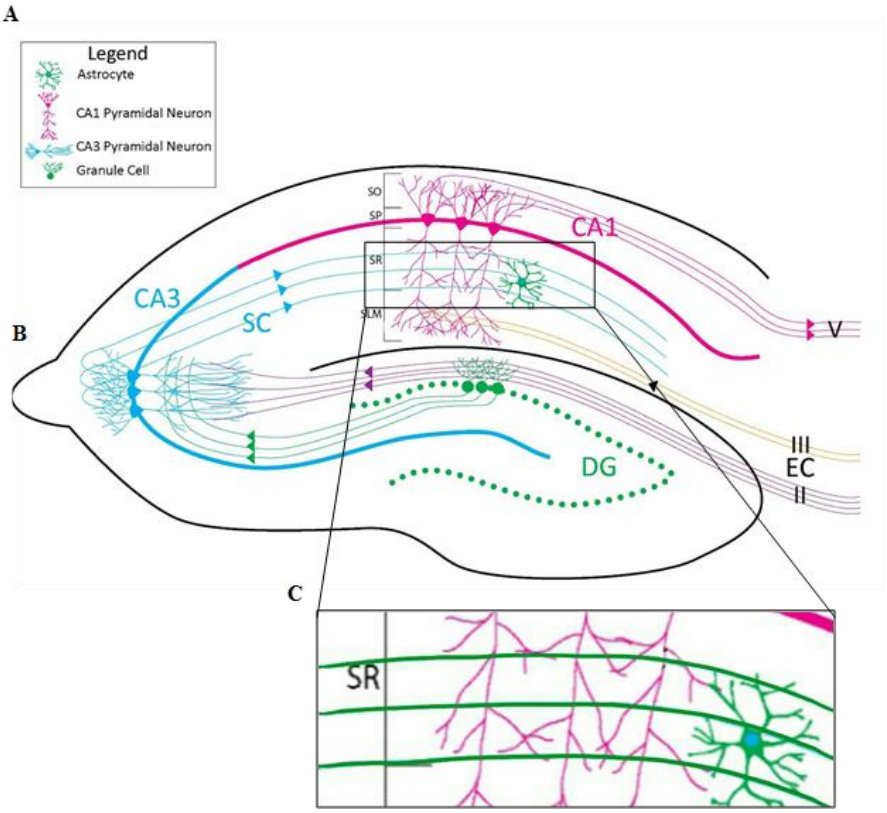

Figure 2.4. Immunostaining of excitatory and inhibitory with vGlut1 and GAD65, respectively. (A) Figure legend. (B) Coronal section of hippocampus depicting pathway from CA3 to CA1. (C) Presynaptic terminals: Schaffer collateral axons in the SR region are shown in green depicting the v-Glut positive excitatory terminals.

Dendritic spine analysis

Thy1-GFP-CRE-ERT2-GFAP-ephrinB1^{Flox} (KO) animals were anesthetized with isofluorine and transcaridaly perfused with 4% paraformaldehyde in 0.1 M phosphate-buffered saline (PBS), pH 7.4 as shown previously (figure 2.3). Brains were post-fixed for 2h in 4% paraformaldehyde/0.1 M PBS and 100 μm coronal sections were cut with a vibratome. No staining was required as the Thy1-GFP-CRE-ERT2-GFAP-ephrinB1^{Flox} (KO) animals possess genetic GFP which causes their neurons to fluorescence. Confocal

images were collected utilizing Zeiss 510 confocal microscope using 63x water-immersion objective. High resolution 1024x1024 pixel format series were collected at 1-μm intervals in the X-Y plane. The obtained images were analyzed using Neurolucida 360 software (MBF Bioscience). We loaded each z-stack onto the Neuroleucida program (Figure 3.3 A). Through the program, we labeled each dendrite (Figure 3.3 B), we then set parameters for the program to detect the dendritic spines; we set the program to detect all protrusions within 2μm of our labeled dendrite, with minimum height 0.2 μm, and minimum count was 15 voxels. We checked to assess if all spines visually present were appropriately labeled by the program. After ensuring all spines were labeled (figure 3.3 C), we analyzed the 3D structures to measure length of spines and density of spines, i.e. number of spines/10 μm dendrite.

Results

Effect of ephrin-B1 KO in astrocytes on excitatory and inhibitory synapses in SR region of the CA1 Hippocampus

In this experiment, tamoxifen injections were administered to P14 knockout (KO, ERT2-Cre^{GFAP} ephrin-B1^{flox}) and wildtype (WT, ERT2-Cre^{GFAP}) littermates for five consecutive days (Figure2.1-2.2). Seven days after the final injection, P28 animals were transcranialy (Figure 2.3) perfused and coronal sections, 100µm thick, were collected and stained to identify hippocampal excitatory and inhibitory synapses. Glutamatergic excitatory synapses were identified using vesicular glutamate transporter 1 (vGlut1, 1mg/4ml; 482400; Invitrogen) antibody, while inhibitory synapses were identified with glutamic acid decarboxylase (GAD65, 10µg/ml; 559931; BD Pharmingen) antibody. Images from two KO tamoxifen-treated ERT2-Cre^{GFAP} ephrin-B1^{flox} (N=2) and two WT tamoxifen-treated ERT2-Cre^{GFAP} animals (*N*=2). A total of 9 z-stack high resolution optical sections (1024x1024 – pixel format) was obtained of the stratum radiatum (SR) of the CA1 hippocampus, at 1µm steps, using a Leica Sp5 confocal microscope. FIJI ImageJ was used to analyze images and count number of excitatory and inhibitory synapses.

Our preliminary results indicate that both KO mice showed an increase in excitatory synapses in the CA1 hippocampus in comparison to number of excitatory synapses in the WT animals. The first KO mouse had an average of 4.95 puncta/10µm^2 (*M*= 4.59 puncta/10µm^2, *SD* = 0.23) and the second KO mouse had an average of 4.05 puncta/10µm^2 (*M* = 4.05 puncta/10µm^2, *SD* = 0.25). Meanwhile, the first WT animal had an average of 1.99 puncta/10µm^2 (*M* = 1.99 puncta/10µm^2, *SD* = 0.11) and the second WT animal had an average of 1.83 puncta/10µm^2 (*M* = 1.83 puncta/10µm^2, *SD* = 0.12),

shown in Figure 3.1 B. A two-way ANOVA was ran to check if there was a difference between KO and WT mice and between mouse 1 and mouse 2 in each condition. We found that there was no difference between mouse 1 and mouse 2 in each condition, F (4.42) < F_{crit} (161.45); however, p-value=0.28, therefore result is not statistically significant. We found that there was a significant difference, p = 0.03, between the KO and WT conditions F (266.03) > F_{crit} (161.45). We will repeat the experiment adding more animals to confirm the preliminary findings. Furthermore, we compared two KO animals and two WT animals with KO and WT animals at P70-P90. We used data previously obtained by lab members from SR region of CA1 hippocampus in adult P70-P90 animal to make the comparison. The adult KO animals also had an increase in vGlut1 levels in comparison to WT mice, the data was analyzed by running one-way ANOVA and the difference between KO and WT mice was found to be statistically significant p <0.01 (Figure 3.1 D).

The number of inhibitory synapses, marked by GAD65, in the SR region of the CA1 of the hippocampus for the same mice was also measured. The first KO mouse had an average of 1.70 puncta/10μm^2 (M = 1.70 puncta/10μm^2, SD = 0.15) and the second mouse showed average of 2.24 puncta/10μm^2 (M = puncta/10μm^2, SD = 0.22). WT mice showed an average of 3.53 puncta/10μm^2 (M = 3.53 puncta/10μm^2, SD = 0.22) for the first mouse and 5.97 puncta/10μm^2 (M = 5.97 puncta/10μm^2, SD = 0.38) for the second mouse. Two-way ANOVA was performed to compare differences between KO and WT conditions, as well as differences between the two mice in each condition. There was no difference between the two animals compared in each condition, F (2.46) < F_{crit} (161.45) with p = 0.361. We also saw no statistically significant difference, p = 0.20, between the

KO and WT mice F (8.56) < F_{crit} (161.45). We will repeat the experiment adding more animals to confirm the preliminary findings. We also compared our results to the previously obtained results from P70-P90 mice. In the P70-P90 animals, the number of inhibitory synapses, GAD65 positive, in KO mice was not significantly different from the number of inhibitory synapses in WT mice.

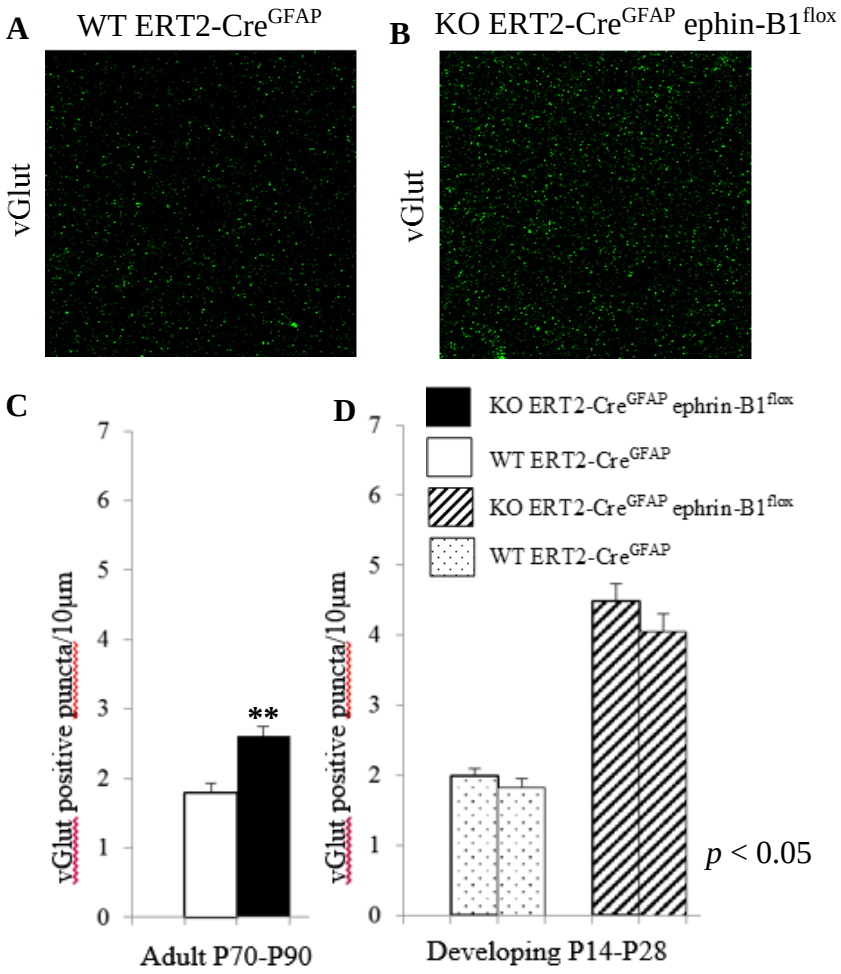

Figure 3.1. Quantification of vGlut1 puncta in adult (P70-P90) and developing hippocampus (P14-P28) of KO and WT animals (A) vGlut1 puncta P28 WT (B) vGlut1 puncta P28 KO (C) Quantification of vGlut1 positive puncta in the SR of P70-P90 WT (5) and KO (5), $^{**}p < 0.01$. (B) Quantification of vGlut1 positive puncta in P28 KO (N =2) and WT (N=2) mice. Two-way ANOVA showed that the differences between WT and KO were statistically significant, $p < 0.05$.

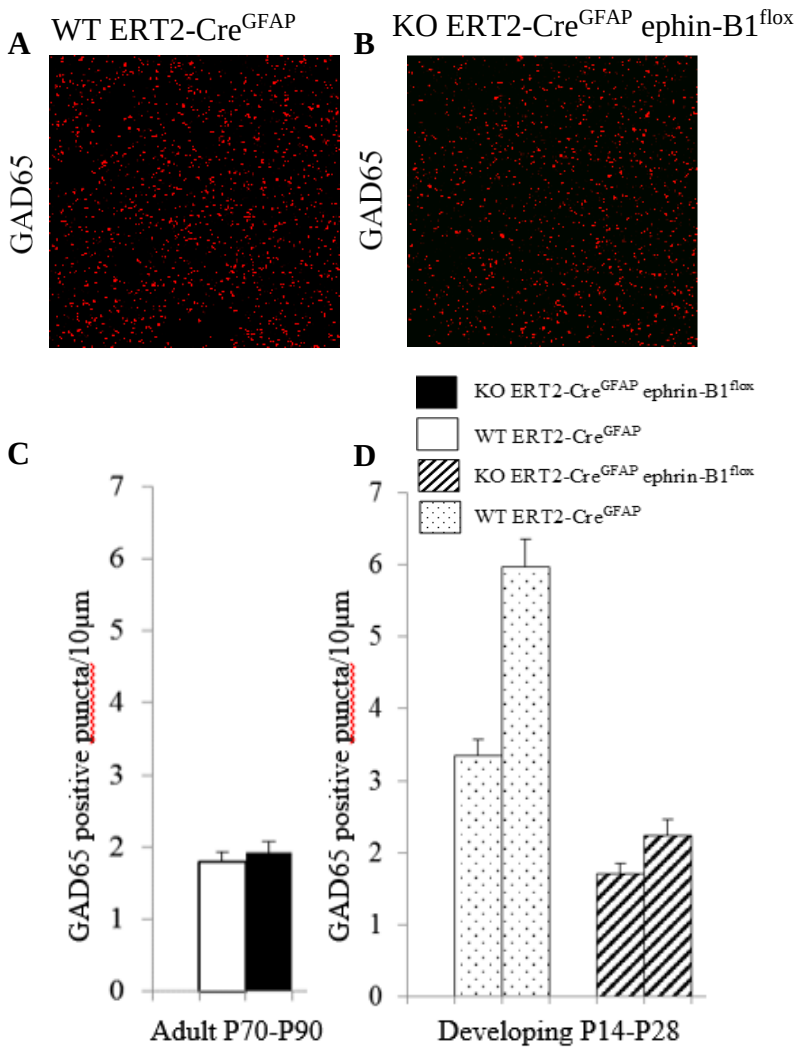

Figure 3.2 Quantification of GAD65 puncta in adult (P70-90) and developing (P14-P28) hippocampus of KO and WT animals. (A) GAD65 puncta P28 WT (B) GAD65 puncta 28 KO (C) Quantification of GAD65 positive puncta in the SR of P70-P90 WT (5) and KO (5), $^{**}p < 0.01$. (B) Quantification of GAD65 positive puncta in 28 KO (N =2) and 28 WT (N=2). Two-way ANOVA showed no significant difference between WT and KO.

Astrocytic ephrin-B1 KO effect on development and morphology of spines in P14-P28 mice.

KO tamoxifen-treated Thy-GFP-ERT2-Cre^{GFAP} ephrin-B1^{flox} and WT tamoxifen-treated Thy1-GFP-ERT2-Cre^{GFAP} animals (see protocol in figure 2.1 and 2.2) were tanscardially perfused (figure 2.3) and coronal sections, 100μm thick, were collected. These animals are genetically modified to express GFP in their genome, causing their neurons to emit fluorescence without use of immunohistochemistry. Confocal images were collected as z-stacks at 1-μm intervals in the X-Y plane using LSM 510, Carl Zeiss confocal microscope with 63x water-immersion objective. Images were analyzed using Neurolucida360 program to determine spine length, and spine density - i.e. number of dendritic spines per 10μm of dendrite length. Genotype was revealed after images were collected and analyzed. Unfortunately, in this experiment both mice that expressed Thy1-GFP gene were identified as KO animals. Future studies will analyze more animals, including WT and KO mice.

In order to analyze the spine length and density z-stacks of confocal images were uploaded onto Neuroleucida360 software (Figure 3.3 A). The dendrites were labeled (Figure 3.3 B), then the program was set to detect all protrusions within 2μm of the labeled dendrite, with minimum height 0.2 μm, and minimum count was 15 voxels. After all spines were appropriately labeled (Figure 3.3C), the program was used to run analysis on spine length and density.

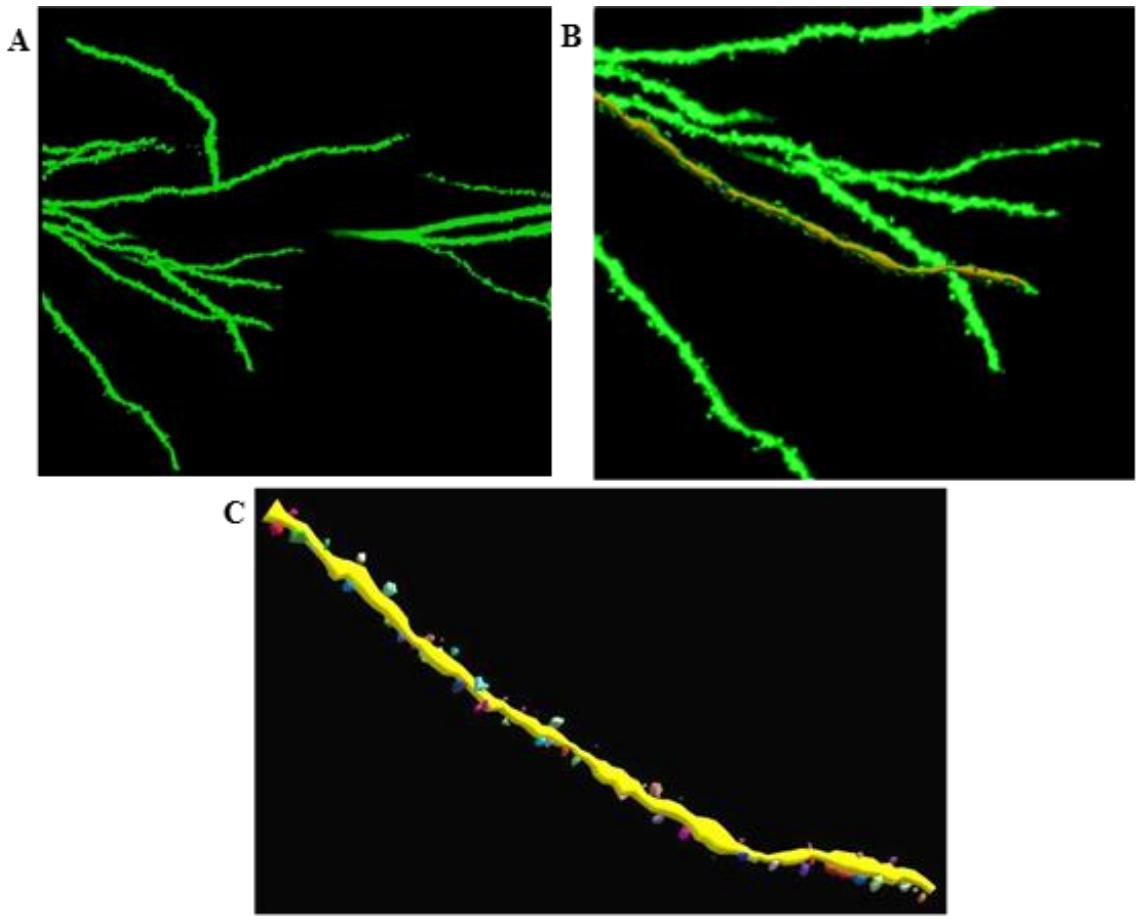

Figure 3.3. Labeling of dendrites and dendritic spines to analyze spine morphology (A) Dendrites from the striatum radiatum region of the hippocampus. (B) Using Neurolucida 360 software, a labeling is superimposed on the dendrite to measure its length and mimic its morphology in order to measure spines attached to it. (C) A clear image of the 3D structure of the dendrite and its labeled spines, produced by Neurolucida360.

Images from two KO tamoxifen-treated Thy-GFP-ERT2-Cre^{GFAP} ephrin-B1^{flox} were used in this analysis, and spines from dendrites were analyzed for each animal. Analysis was performed on spine length and spine density, spines per 10 µm of dendrite. We compared our data with data previously obtained from KO animals at age P70-P90; in these experiments dendrites were labeled in KO tamoxifen-treated ERT2-Cre^{GFAP} ephrin-B1^{flox} and WT tamoxifen-treated ERT2-Cre^{GFAP} using DiI staining, similar to Nikoulapoulou (2016). The P14-P28 KO average spine lengths were 1.85 (M = 1.85, SD = 0.06) for mouse 1, and 1.94 (M = 1.94, SD = 0.04) for mouse 2; the lengths were comparable to the average spine length found in P70-P90 mice, (M = 2.04, SD = 0.01) (Figure 3.4 A, B). The average spine density, spines per 10 µm of dendrite, was also calculated for the dendrites in each animal and compared to the values of the P70-P90 KO animals (Figure 3.5). The average spine density was 7.74 spines/10 µm in dendrites from mouse 1 (M = 7.74, SD = 1.08), and 6.28 spines/10 µm in dendrites from mouse 2 (M = 6.28, SD = 0.55). The values for the spine density in the adult KO animals were greater (M = 11.28, SD = 0.36). However, this could be due to the difference in age between the animals, the younger animals may have less spines merely because they are younger and still growing. Therefore, we will need to add WT animals to our age group to determine if there is a significant effect for ephrin-B1 on spine density at this age in the KO mice.

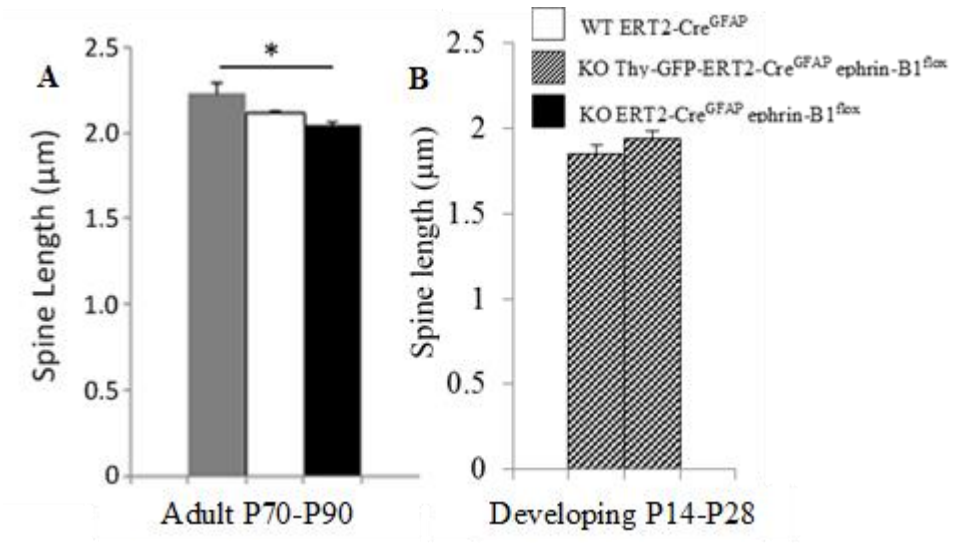

Figure 3.4. Effects of ephrin-B1 KO in astrocytes on spine length (A) Spine length in P70-P90 WT tamoxifen-treated ERT2-Cre^{GFAP} and KO ERT2-Cre^{GFAP} ephrin-B1^{flox}, spine length was reduced in KO mice, $p < 0.05$. (B) Spine length in two tamoxifen-treated P14-P28 KO Thy-GFP-ERT2-Cre^{GFAP} ephrin-B1^{flox} animals.

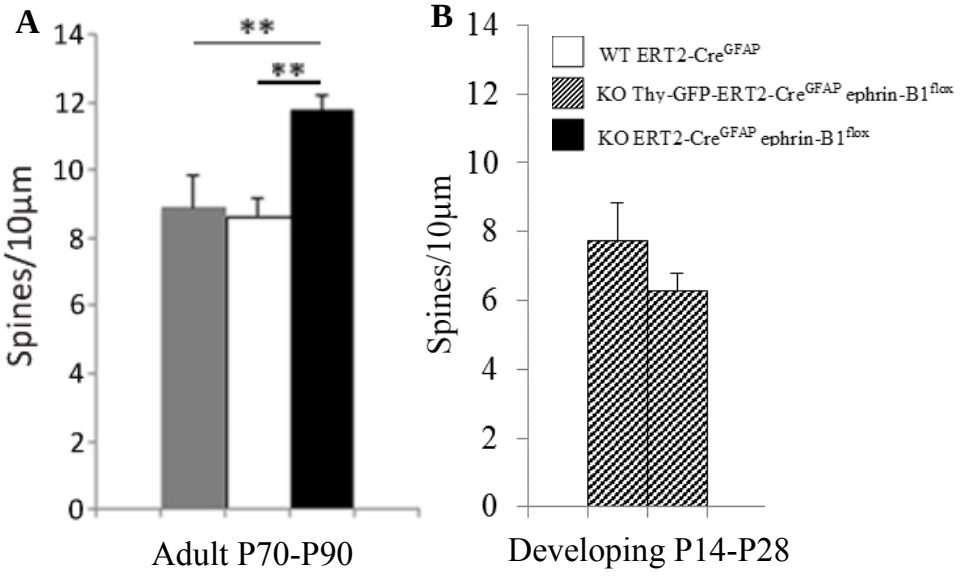

Figure 3.5. Effect of ephrin-B1 KO on spine density (A) Spine density in P70-P90 WT tamoxifen-treated ERT2-Cre^{GFAP} and KO ERT2-Cre^{GFAP} ephrin-B1^{flox}, spine density was significantly increased in KO mice, $p < 0.01$. (B) Spine density in P14-P28 KO mice.

Discussion

In this project, we aimed to analyze the effects of astrocytic ephrin-B1 knockout on excitatory signaling in the stratum radiatum (SR) layer of the CA1 hippocampus during development. We hypothesized that ephrin-B1 is involved in pruning of excitatory synapses during development, and such pruning is important for dendritic spines to become mature. Thereby, we expected the ephrin-B1 KO mice to show increased numbers of excitatory synapses, vGlut1 positive, in comparison to our WT mice. Yet, we did not expect to see a change in the inhibitory synapses, GAD 65. Furthermore, in comparison to WT, we expected KO mice to have increased spine density, due to the lack of pruning, as well as increased spine length, characteristic of immature spine morphology. Consistent with our hypothesis, two P14-P28 tamoxifen treated ERT2-Cre^{GFAP} ephrin-$B1^{flox}$ (KO) showed an increase in the number of excitatory synapses, vGlut1 positive, in comparison to two P14-P28 tamoxifen treated ERT2-Cre^{GFAP}(WT), $p < 0.05$ (Figure 3.1 A, B and C). However, there was no significant increase in the inhibitory, GAD65 positive, synapses (Figure 3.2 A, B and C). Future studies will analyze more animals, including WT and KO mice to confirm the finding.

Previous experiments in our lab showed a correlation between an increase in astrocytic ephrin-B1 in the SR CA1 of hippocampus, following Traumatic Brain Injury (TBI), and a decrease in excitatory synapses in the same region (Nikolakopoulou et al., 2016). Thereby suggesting that astrocytic ephrin-B1 may play a role in modification of synapses in this region. Similarly, our findings suggest a possible role of ephrin-B1 in modification of synapses during development, where deficiency in ephrin-B1 caused an increase in the excitatory synapses, $p < 0.05$; suggesting that ephrin-B1 may be pruning

away the excitatory synapses. Furthermore, our findings were consistent with previous findings from our lab, which showed a statistically significant increase in excitatory synapses upon deletion of ephrin-B1 in adult astrocytes, age P70-P90, $p < 0.01$. These studies also found no significant change in inhibitory synapses.

The other part of our hypothesis was that the pruning of synapses by ephrin-B1 during development is contributing to maturation of the dendritic spines that continue to exist (Figure 1.3). Analysis of dendritic spines was performed on P14-P28 tamoxifen-treated Thy-GFP-ERT2-Cre^{GFAP} ephrin-B1^{flox} (KO) mice, and showed average spine lengths 1.84 ± 0.06 and 1.94 ± 0.04 which were comparable to the average spine length in the adult KO animals, 2.04 ± 0.01 (Figure 3.5). Future studies will perform a comparison between P14-P28 KO and WT to determine if such effect is in fact present. Similarly, conclusions cannot be drawn about the effect of ephrin-B1 on spine density in the KO animals, the average for spine density in the two KO mice observed were 7.74 spines/10µm ± 1.08 and 6.28 spines/10µm ± 0.55, which were less than average spine density, 11.28 spines/10µm ± 0.36, observed in previous experiments by other lab members in the adult KO mice. This decrease could be due to the fact that the mice are younger and still growing, or it could be about the extent of synapse pruning at that age; conclusions cannot be drawn until we have observed WT animal spine density at the P14-P28 and compared the KO and WT spine densities.

The increase in excitatory synapses, particularly at the pre-synaptic side, in the astrocytic ephrin-B1 KO may suggests that ephrin-B1 is essential for pruning or maintaining the number of excitatory synapses during development. Deleting ephrin-B1 during development caused an increase in the number of vGlut1 positive puncta while the

GA65 puncta, labeling inhibitory synapses, stayed the same. This suggests that astrocytic ephrin-B1 may be involved in removing some of the excitatory synapses that are not removed in ephrin-B1 KO mice. In Segura et al (2007) inactivation of neuronal ephrin-B1 in vitro, by transfecting neurons with EphrinB1ΔC, caused an increase in spine density, and length. EphrinB1ΔC was dimerizing the EphB receptors, thereby blocking the endogenous ephrin-B1 from binding to its designated receptors. The studies showed that ephrin-B1 inactivation was associated with an increase in immature synapses in the knockout neurons when compared to the wildtype neurons. In other studies, triple mutant hippocampal neurons for EphB1/B2/B3 lacked mature spines, instead they expressed long filopodia-like protrusions which lack polymerized actin. Furthermore, these mutant neurons formed synapses at the shaft of the dendrite, whereas WT neurons formed synapses at the dendritic spines of the dendrite (Henkenmeyer et al., 2003). These studies along with data we have discussed in this project lead us to think that astrocytes may be pruning immature synapses containing unoccupied EphB receptors through its interactions with astrocytic ephrin-B1 during development and consequently causes decrease in excitatory synapses. These effects of ephrin-B1 could be playing a major role in the fine-tuning of the hippocampal circuits in the SR CA1 region during development, where pruning away an excess of immature excitatory synapses helps to maintain mature synapses. However, future spine analysis and comparisons between P14-P28 KO and WT animals are essential to test this hypothesis.

In future experiments, we will continue to analyze the effect of ephrin-B1 deletion on P14-P28 animals, we will be adding more animals to each of the P14-P28 tamoxifen treated ERT2-Cre^{GFAP}(WT), which is our control group, and P14-P28 tamoxifen treated

ERT2-Cre^{GFAP} ephrin-B1^{flox} (KO) groups. The additions of more animals to our samples will allow us to draw conclusions on the plausible role of ephrin-B1 in the pruning of excitatory synapses. We also plan on analyzing more animals for each of the tamoxifen treated Thy-GFP-ERT2-Cre^{GFAP} ephrin-B1^{flox} KO and tamoxifen treated Thy1-GFP-ERT2-Cre^{GFAP} WT mice. These experiments will allow us to draw conclusions on the effect of ephin-B1 on spine density and morphology, and consequently on maturation of the dendritic spines. In this project, we did not analyze the volume of the dendritic spines nor classified the spines based on morphology, e.g. mushroom-like (mature) versus filopodia-like (immature); therefore, in future experiments we will perform this analysis as well. These studies will tell more on the role of ephrin-B1 in astrocyte-mediated pruning of synapses, and how it contributes to the refinement of the hippocampal circuits; which may help us to understand the mechanisms underlying learning and memory.

References

Bush JO, Soriano P. (2009). Ephrin-B1 regulates axon guidance by reverse signaling through a PDZ- dependent mechanism. *Genes Dev 23*(13): 1586-1599.

Egea, J., & Klein, R. (2007). Bidirectional Eph–ephrin signaling during axon guidance. *Trends In Cell Biology*, 17(5), 230-238.

Ethell IM, Irie F, Kalo MS, Couchman JR, Pasquale EB, Yamaguchi Y. (2001) EphB/syndecan-2 signaling in dendritic spine morphogenesis. *Neuron 31* (6): 1001–13.

Gage, G. J., Kipke, D. R., Shain, W. (2012). Whole Animal Perfusion Fixation for Rodents. *Journal of Visualized Experiments* (65), e3564

Gale NW, Holland SJ, Valenzuela DM, Flenniken A, Pan L, Ryan TE, Henkemeyer M, Strebhardt K, Hirai H, Wilkinson DG, Pawson T, Davis S, Yancopoulos GD (1996). Eph receptors and ligands comprise two major specificity subclasses and are reciprocally compartmentalized during embryogenesis. *Neuron*. 17(1): 9-19.

Gottschalk et al., W.A. Gottschalk, H. Jiang, N. Tartaglia, L. Feng, A. Figurov, B. (1996). Signaling mechanisms mediating BDNF modulation of synaptic plasticity in the hippocampus. *Learn Mem*., (6): 243–256.

Guellmar et al., A. Guellmar, J. Rudolph, J. Bolz. (2009) Structural alterations of spiny stellate cells in the somatosensory cortex in ephrin-A5-deficient mice *J. Comp. Neurol.* (517): 645–654.

Harris KM. (1999). Structure, development, and plasticity of dendritic spines. *Curr Opin Neurobiol* 9(3), 343-348.

Haina, Q., Noberini, R., Xuelu, H., Jiahai, S., Pasquale, E. B., & Jianxing, S. (2010). Structural Characterization of the EphA4-Ephrin-B2 Complex Reveals New

Features Enabling Eph-Ephrin Binding Promiscuity. *Journal Of Biological Chemistry*, 285(1), 644-654

Henderson JT, Georgiou J, Jia Z, Robertson J, Elowe S, Roder JC, Pawson T. (2001). The receptor tyrosine kinase EphB2 regulates NMDA-dependent synaptic function. *Neuron* 32(6):1041-1056.

Henkemeyer M, Itkis OS, Ngo M, Hickmott PW, Ethell IM. (2003). Multiple EphB receptor tyrosine kinases shape dendritic spines in the hippocampus. *J Cell Biol* 163(6):1313-1326.

Hruska, M., & Dalva, M. B. (2012). Ephrin regulation of synapse formation, function and plasticity. *MCN: Molecular & Cellular Neuroscience,* 50(1), 35-44.

Kao, T., Law, C., & Kania, A. (2012). Eph and ephrin signaling: Lessons learned from spinal motor neurons. Seminars In Cell & Developmental Biology, 23(1), 83-91

Kayser, M. S., McClelland, A. C., Hughes, E. G., & Dalva, M. B. (2006). Intracellular and Trans-Synaptic Regulation of Glutamatergic Synaptogenesis by EphB Receptors. *Journal Of Neuroscience*, 26(47), 11.

Marler et al., K.J. Marler, E. Becker-Barroso, A. Martinez, M. Llovera, C. Wentzel, S. Poopalasundaram, R. Hindges, E. Soriano, J. Comella, U. Drescher. (2008) A TrkB/EphrinA interaction controls retinal axon branching and synaptogenesis. *J. Neurosci.,* (28): 12700–12712

Murai KK, Nguyen L., Irie F, Yamaguchi Y, & Pasquale, EB. (2003). Control of hippocampal dendritic spine morphology through ephrin A3/EphA4 signaling. *Nature Neurosci* 6; 153–160.

Nikolakopoulou AM, Koeppen J, Garcia M, Leish J, Obenaus A, Ethell IM (2016). Astrocytic Ephrin-B1 Regulates Synapse Remodeling Following Traumatic Brain Injury. *ASN Neuro* 1–18.

Grunwald IC, Korte M, Adelmann G, Plueck A, Kullander K, Adams RH, Frotscher M, Bonhoeffer T, & Klein R. (2004). Hippocampal plasticity requires postsynaptic ephrinBs. *Nature Neurosci* 7(1), 33-40.

Segura, I., Essmann, C. L., Weinges, S., & Acker-Palmer, A. (2007). Grb4 and GIT1 transduce ephrinB reverse signals modulating spine morphogenesis and synapse formation. *Nature Neuroscience,* 10(3), 301-310.

Sloniowski S, Ethell IM. (2012). Looking forward to EphB signaling in synapses. *Semin Cell Dev Biol* 23(1):75-82.

Takasu MA, Dalva MB, Zigmond RE, & Greenberg ME. (2002). Modulation of NMDA receptor-dependent calcium influx and gene expression through EphB receptors. *Science* 295(5554), 491-495.

Xu, Q., Mellitzer, G., Robinson, V., & Wilkinson, D. G. (1999). In vivo cell sorting in complementary segmental domains mediated by Eph receptors and ephrins. *Nature*, 399(6733), 267.

Xu NJ, Henkemeyer M. (2012). Ephrin reverse signaling in axon guidance and synaptogenesis. *Semin Cell Dev Biol* 23(1):58-64.